

SINGLE LLRF FOR MULTI-HARMONIC BUNCHER*

N. Usher^{†1}, S. Zhao, D. Morris, J. Brandon, D. Alt

Facility for Rare Isotope Beams (FRIB), East Lansing, MI 48824, USA

¹also at, Ionetix Corporation, Lansing, MI 48911, USA

Abstract

In this paper, a unique low level radio frequency (LLRF) controller designed for a multi-harmonic buncher (MHB) is presented. Different than conventional designs, the single LLRF output contains three RF frequencies (f_1 , $f_2 = 2*f_1$, $f_3 = 3*f_1$) and is fed to a wide-band amplifier driving the MHB. The challenge is while driving f_1 , due to the non-linearity of the amplifier, the f_2 and f_3 terms will also be generated and will couple into the control of these two modes. Hence an active cancellation algorithm is used to suppress the nonlinear effect of the amplifier. It is demonstrated in a test that the designed LLRF is able to control the amplitude and phase of the three modes independently.

INTRODUCTION

The re-accelerator (ReA3) at the National Superconducting Cyclotron Laboratory (NSCL) is mainly running at 80.5 MHz RF. The existing multi-harmonic buncher (MHB) in ReA3 runs at 80.5 MHz, 161 MHz and 241.5 MHz RF (latter not actively used) [1]. To achieve an increased separation of the beam bunches and minimization of bunch lengths desired for many types of experiments that use time of flight measurements, a lower frequency prebuncher (also an MHB) is designed [2]. To be compatible with the existing ReA3, the fundamental frequency (f_1) of the prebuncher is chosen to be 16.1 MHz. The second harmonic ($f_2 = 32.2$ MHz) and the third harmonic ($f_3 = 48.3$ MHz) will also be used.

In the rest of the paper, the RF design for the prebuncher including the resonant circuit, RF input sampling and output synthesis, as well as the control algorithm is described. Following, the bench test verification is presented as a proof of concept. Finally, the experimental results are given followed by conclusions.

RF DESIGN

Normally for MHB the control of each frequency component is done with a dedicated low level radio frequency (LLRF) controller, e.g. in the ReA3 MHB and FRIB MHB [3]. Three LLRF controllers and amplifiers will be needed. Since the frequencies are close enough, one wide band power amplifier could be used to amplify all three frequencies. Also with the more powerful field programmable gate array (FPGA) chip, it is possible to accommodate the logics, including digital mixing, filtering and feedback control, for all three harmonics in one LLRF controller. In

this paper, such a unique RF system is designed and implemented.

Resonant Circuit

An effective way to achieve high voltage across the buncher electrodes is using resonant coaxial structures [1]. For this application, two resonant structures were used in parallel. A first coaxial cable was resonated at 16.1 MHz (f_1) and 48.3 MHz (f_3), and a second cable was resonated at 32.2 MHz (f_2). Figure 1 shows a schematic of the RF circuit. The lumped elements represent the feedthrough connections and electrode gap capacitance. Note: the resistors in the schematic were used to de-Q the circuit for simulations only, and were not used in the actual circuit. Good isolation was achieved by carefully selecting the lengths of cables A and B.

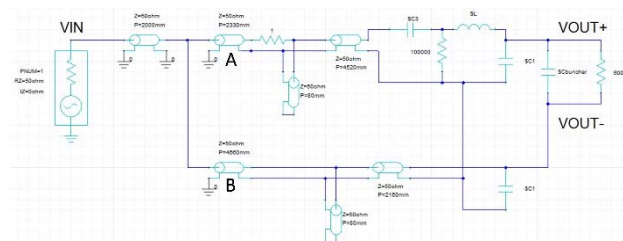


Figure 1: Schematic for RF system.

Each resonant structure includes a roughly quarter wavelength section (or odd multiple thereof) of 7/8” air-dielectric coaxial cable (RFS HCA78-50J) that was coiled to save space. A piece of 3-1/8” rigid transmission line was used as an input-tuning section, which consisted of a sliding short (for setting the resonant frequency) and a slot tuned input port. Figure 2 shows the input-tuning sections in the final installation.

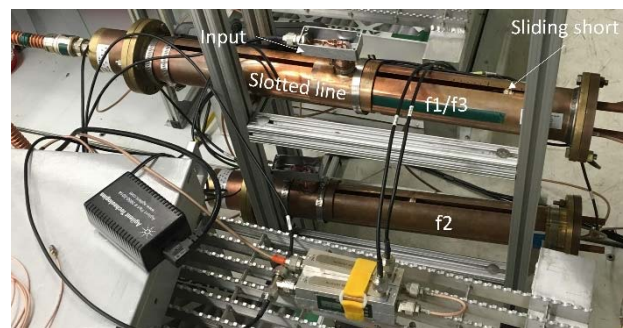


Figure 2: Input-tuning sections of coaxial resonators.

All three frequencies were simultaneously matched with return loss better than -9 dB, as shown in Figure 3.

* Work supported by Michigan State University, National Science Foundation: NSF Award Number PHY-1102511.

[†]usher@frib.msu.edu



Figure 3: Input return loss.

RF Inputs Sampling and Processing

As described in previous section, there are two resonant structures. Each has a cavity pickup that feeds one LLRF input channel. Signal on Channel 1 contains f_1 and f_3 ; signal on Channel 2 contains only f_2 . Same as the LLRF for FRIB, non-IQ direct sampling is adopted. The sampling frequency is chosen as 31.19375 ($=16.1 \times 31/16$) MHz, i.e. f_1 will be sampled 31 times over 16 waveforms; 32 waveforms for f_2 and 48 waveforms for f_3 correspondingly. After sampling, each frequency component is mixed individually with a digital mixer (at its own frequency), then filtered with a cascaded integrator-comb (CIC) filter and a low-pass filter to generate the I/Q pair.

RF Output Synthesis

In order to generate all three frequencies from a single output digital-to-analogue converter (DAC), the sampling frequency must be a multiple of all of the RF frequencies. For this project, the DAC sampling frequency was set to $16 \times f_1$. Since the output is oversampled, the I/Q output has not enough points, so additional sample points must be generated. To generate the additional points, a coordinate rotation digital computer (CORDIC) algorithm converts the I/Q pair to amplitude/phase. The amplitude is saturated and fixed phase offsets of 0° , 22.5° , 45° , and 67.5° are added before the four amplitude/phase pairs are converted back to I/Q (22.5° and 67.5° are not required for f_2). This gives all 16 points necessary for output generation. Since the DAC sample clock is $16 \times f_1$, samples for f_1 are 22.5° apart, samples for f_2 are 45° apart, and samples for f_3 are 67.5° apart. To produce each DAC sample, the samples from f_1 , f_2 , and f_3 are summed. The saturation limit per channel in the amplitude/phase domain prevents overflow when the frequencies are summed.

Control Algorithm

A special advanced control algorithm called active disturbance rejection control (ADRC) is used at NSCL for microphonics suppressing since 2011 [4]. The ADRC is well known for its capability of decoupling system variables, e.g. amplitude and phase in the superconducting cavity control. So it naturally fits into this application, where decoupling of individual frequency component is desired.

In this application, there is an independent ADRC process for each output frequency (the control loop for each frequency does not use feedback from either of the other

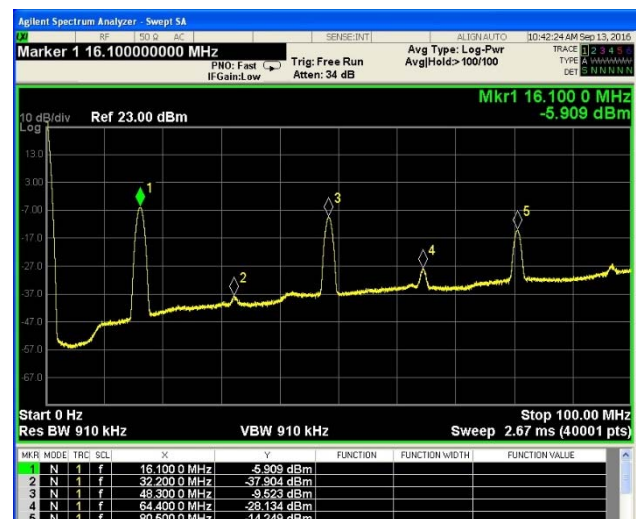
frequencies). Each control loop produces an I/Q output. Different from [5], I/Q control rather than amplitude and phase control is adopted, due to the simplicity of RF output synthesis in the I/Q domain. A zero-order ADRC is used due to the fast response of the MHB compared to the superconducting cavities.

BENCH TEST

To test the above LLRF design, a bench test was first conducted to verify the concept. The test setup is described as follows. The LLRF controller drives a wide band power amplifier (EMPOWER 2160-BBS2E3DKM, 20~125 MHz, 100 W). The output of the amplifier goes through a high power directional coupler (NARDA 3020A) and finally into a dummy load (> 300 W). The forward coupling port of the high power directional coupler is connected to a low power directional coupler (Mini-Circuit ZFDC-10-182+) and then a two way splitter (Mini-Circuits ZFRSC-2050) which feeds the two cavity input channels (f_1/f_3 , f_2) of the LLRF controller as feedback. The forward coupling port of the low power directional coupler is connected to a spectrum analyser for monitoring.

Open Loop

Figure 4 shows the spectrum of the open loop RF pickup signal while driving f_1 only. As expected, the third harmonic is significant compared to f_1 due to the nonlinearity of the power amplifier. Note: the plot includes the high pass frequency response of the high power directional coupler (f_3 is actually 12.6 dB lower than f_1 when adjusted for the coupler response).

Figure 4: Spectrum of the open loop RF pickup signal while driving f_1 only.

Closed-Loop

To check the effectiveness of the proposed control algorithm, f_3 is driven in closed-loop with a set-point of 0. As seen in Figure 5, the f_3 component from the amplifier is suppressed by 19.9 dB.

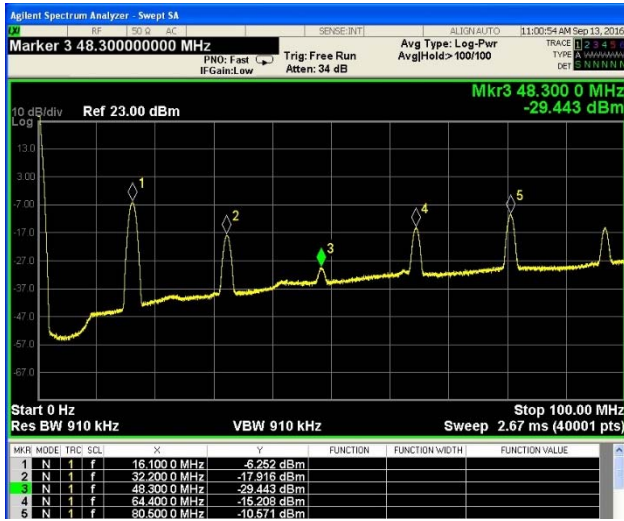


Figure 5: Spectrum of the RF pickup signal when f_1 and f_2 are in closed-loop (set-point of f_3 is zero).

EXPERIMENTAL RESULTS

In February 2016, an experiment using the prebuncher was carried out in ReA3. The third harmonic ($f_3 = 48.3$ MHz) was not used for beam bunching in this experiment, and was driven to 0 amplitude. The amplitude and phase set-points for f_1 are 335 V and 22° ; the amplitude and phase set-points for f_2 are 35 V and 202° . As shown in Figure 6, nearly 85% of the particles are concentrated in the main beam bunch. Some residual bunches can still be seen at 80.5 MHz rate. Figure 7 shows the operator interface used during the experiment.

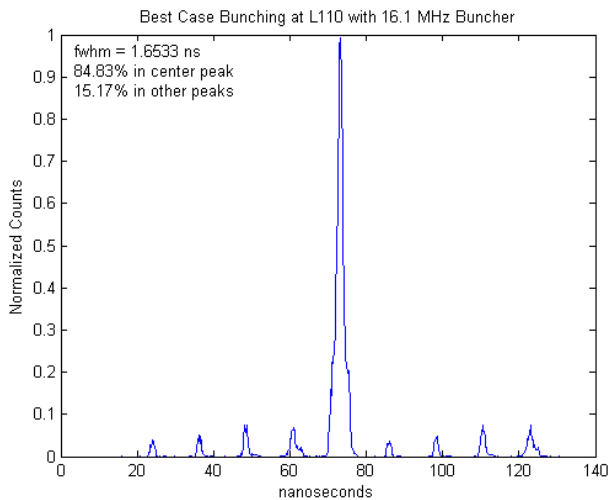


Figure 6: Time structure of the beam at the end of ReA3.



Figure 7: Prebuncher CS-Studio OPI.

Table 1 summarizes the control performance of the first two frequencies.

Table 1: Control Performance of f_1 and f_2 .

Error	f_1 (16.1 MHz)	f_2 (32.2 MHz)
Amplitude peak	0.249%	2.775%
Amplitude rms	0.069%	0.756%
Phase peak	0.146°	1.832°
Phase rms	0.066°	0.429°

It is obvious that f_1 terms are very well controlled. The error of the f_2 terms are higher due to the lower signal to noise ratio ($V_1 \sim 10V_2$).

CONCLUSIONS

This unique LLRF design is more cost effective compared to the conventional designs (saves two sets of LLRF controller and amplifier), while providing satisfactory performance.

REFERENCES

- [1] Q. Zhao *et al.*, “Design and Test of Triple-Harmonic Buncher for the NSCL ReAccelerator,” in *Proc. LINAC’08*, Victoria, BC, Canada, Sep. 2008, paper THP069, pp. 948-950.
- [2] D. Alt *et al.*, “Preparatory Investigations for a Low Frequency Prebuncher at ReA,” in *Proc. IPAC’14*, Dresden, Germany, Jun. 2014, paper THPME051, pp. 3342-3345.
- [3] J. Holzbauer *et al.*, “Electromagnetic Design of a Multi-Harmonic Buncher for the FRIB Driver LINAC,” in *Proc. PAC’11*, New York, NY, USA, Mar. 2011, paper TUP091, pp. 1000-1002.
- [4] J. Vincent *et al.*, “On active disturbance rejection based control design for superconducting RF cavities,” *Nucl. Instr. Meth. A*, vol. 643, no. 1, pp. 11-16, 2011.
- [5] S. Zhao *et al.*, “Fixed-point implementation of active disturbance rejection control for superconducting radio frequency cavities” in *Proc. 2013 American Control Conference*, Washington, DC, USA, Jun. 2013, pp. 2693-2698.